1991A&A...247..469N

Astron. Astrophys. 247, 469–475 (1991)

ASTRONOMY AND ASTROPHYSICS

Pollution of P Cygni line profiles by Fe IV and Fe V photospheric absorption in the ultraviolet spectrum of O-type stars

F. Nemry [1,*], **J. Surdej** [1,**], **and A. Hernaiz** [2,***]

[1] Institut d'Astrophysique, Université de Liège, Avenue de Cointe 5, B-4000 Liège, Belgium
[2] Instituto de Astronomia y Fisica del Espacio, CC67–SUC28, Buenos Aires 1428, Argentina

Received October 5, accepted December 3, 1990

Abstract. When visualizing the IUE Atlas of O-Type Spectra from 1200 to 1900 Å (Walborn et al. 1985), one notices immediately that underlying interstellar and photospheric absorption lines do affect significantly both the star continuum and the P Cygni profiles due to resonance line transitions of Si IV, C IV, etc. We report here that the main pollution in the spectral ranges 1270–1500 and 1500–1860 Å is caused by photospheric absorption lines of Fe V and Fe IV, respectively. Making use of the first order moment W_1 of a P Cygni line profile, we show that the effect of this photospheric pollution may lead to systematic errors, exceeding typically 50%, in the determination of mass loss rates. We also emphasize the importance to correct the observed P Cygni line profiles for this pollution when studying the dependence of the physical parameters, terminal velocity, etc. of the stellar winds upon the various classes and types of O stars.

Key words: lines: formation – lines: identification – lines: profile – spectroscopy – stars: mass loss

1. Introduction

The publication by Walborn, Nichols-Bohlin and Panek (1985, referred hereafter as WNP) of an atlas of IUE O-type spectra has provided astrophysicists with a unique tool to study the mass loss phenomena taking place in the atmospheres of early-type stars. Among the various methods proposed for analyzing the P Cygni profiles due to resonance line transitions, the n^{th} order moment technique has proven to be well adapted for a statistical investigation of the properties of stellar winds (Surdej 1983b, 1985; Cerruti-Sola & Perinotto 1985, 1989; Surdej & Hutsemékers 1990). The moment W_n of a P Cygni line profile appears to be the generalization of the equivalent width of an absorption line and gives rise, in the case of expanding atmospheres, to useful astrophysical diagrams similar to the well known curve of growth for the case of static atmospheres. We recall here that, in the optically thin approximation, the moments W_1, W_2 and W_3 are directly related to the mass loss, to the momentum and to the kinetic energy rates of the expanding envelope, respectively (Castor et al. 1981; Surdej 1982, 1983a, 1985). In the process of constructing $W_n - W_{n'}$ diagrams ($n \neq n'$) from measurements of the n^{th} order moments of the P Cygni profiles compiled in WNP, we have experienced serious difficulties in setting unambiguously the level of the local stellar continua. Therefore, in order to identify all interstellar and photospheric absorption lines affecting the continuum spectrum of those early-type stars, we have summed up and averaged the 101 spectra of 98 stars listed in the atlas. It has then become clear that the P Cygni profiles themselves were severely polluted not only by known interstellar lines but also by unidentified photospheric absorption lines. We report here on the identification of these "polluting" lines and also about their effects on the determination of mass loss rates, terminal velocities, etc. as derived from the analysis of observed P Cygni line profiles.

2. Identification of the polluting absorption lines

In order to identify all interstellar lines present in the IUE spectra of O-type stars (see WNP for a detailed description of the spectrograms in their atlas), we decided first to construct different sets of averaged spectra: we chose 2 sets of 50 averaged spectra, 4 sets of 25 averaged ones, etc. Comparison of these independent average spectra led us to the conclusion that, alike the case of well known interstellar lines (cf. compilation in WNP, Table 3), most of the other features seen in the individual spectra were also due to physical lines and not to noise, as it is sometimes believed (compare the two sets of 50 averaged C IV line profiles illustrated in Fig. 1). Furthermore, intercomparison of the above average spectra with the IUE spectrum of SN 1987a (Blades et al. 1988) precludes that the observed absorption features are artefacts caused by the internal flat field calibration of the IUE spectra. As confirmed by Dr. C. Leitherer (private communication), errors in the internal IUE flatfield are anyway not large enough to produce the observed absorption features.

In a second step, we made use of the compilation of atomic wavelengths data by Kelly & Palumbo (1973), by Striganov & Sventitskii (1968) and by Moore (1962, 1967, 1970, 1971, 1975), and could identify some of the lines as being of interstellar or pho-

Send offprint requests to: J. Surdej

* Also, Aspirant au Fonds National de la Recherche Scientifique (Belgium)

** Also, Chercheur Qualifié au Fonds National de la Recherche Scientifique (Belgium)

*** Also, Fellow of the Consejo Nacional de Investigaciones Cientificas y Tecnicas (Argentina)

© European Southern Observatory • Provided by the NASA Astrophysics Data System

1991A&A...247..469N

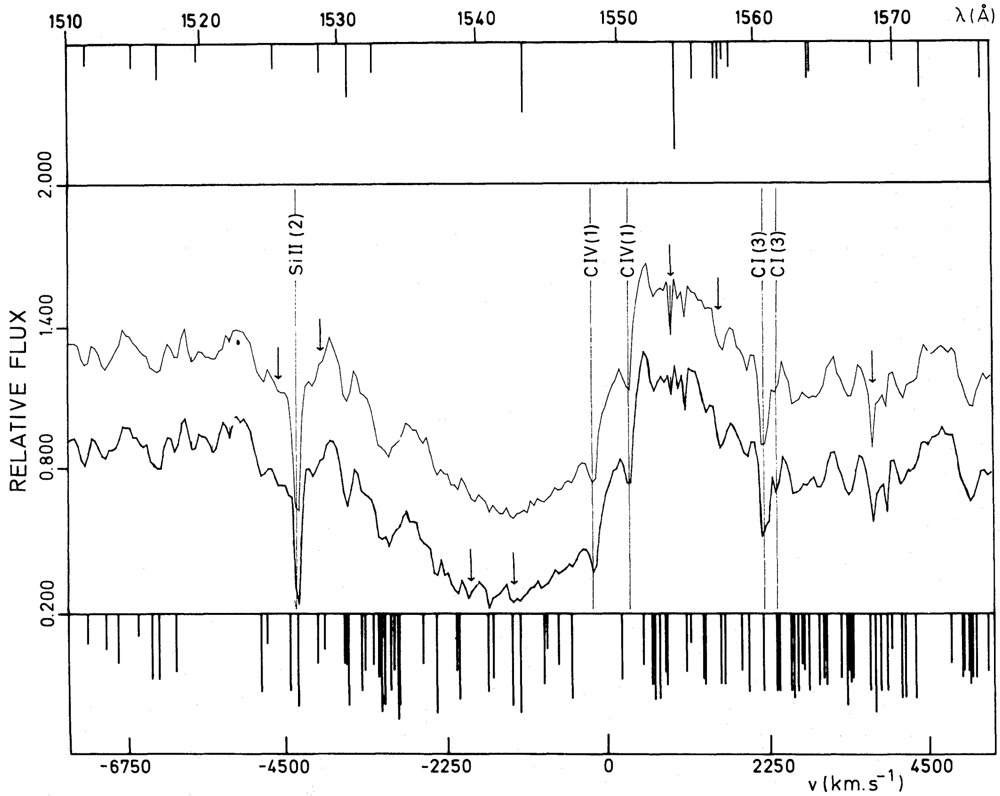

Fig. 1. The upper spectrum illustrates the representative C IV P Cygni line profile for O-type stars as constructed from the average of the 50 first spectra in the WNP atlas. The lowest spectrum was similarly obtained from the average of the 50 next spectra in the atlas. Contamination of the spectra by reseau marks is indicated with arrows. The vertical lines at the top and at the bottom of this figure represent the expected positions and strengths of Fe V and Fe IV lines, respectively (see Text)

tospheric origin but the results were not judged to be very satisfactory because most of the absorption features remained unidentified. We could solve this puzzle thanks to the line identifications reported by Bruhweiler et al. (1981) and Dean & Bruhweiler (1985) for the spectra of the subdwarfs BD+75°325, HD 49798 and BD+28°4211 and of the main-sequence star HD 46202. We could finally complete all our identifications using the lists of experimental wavelengths and predicted relative intensities of Fe V by Ekberg (1975) and of Fe IV by Ekberg & Edlen (1978). A detailed list of line identifications in the whole average spectrum will be published elsewhere (Nemry et al. 1991a). To summarize, we can say that the Fe V lines dominate in the spectral range 1270–1500 Å, while the Fe IV lines are more prominent between 1500 and 1860 Å. In this paper, we concentrate on the identification of the polluting lines located within the P Cygni line profiles due to Si IV, C IV, He II and N IV, which are of general interest for the study of mass loss from O-type stars.

2.1. Si IV λλ *1393*, *1402 Å*

A forest of Fe V lines affects considerably the whole Si IV P Cygni line profile. Fe IV does only contribute marginally to this line pollution. These effects are well illustrated in Figs. 2a and 2b where the vertical lines indicate the positions and strengths of the Fe V (upper part) and Fe IV (lower part) lines. Known interstellar and photospheric absorption lines are also marked in these figures. Figure 2a represents the average Si IV P Cygni line profile for 28 supergiant O-type stars selected from the atlas of WNP. Figure 2b refers to a subsample of 20 main-sequence and dwarf O-type stars, characterized by fainter luminosities and revealing no wind effects. We shall take advantage in Sects. 3 and 4 of this well known Si IV stellar wind – luminosity effect (Walborn and Panek 1984; compare Figs. 2a and 2b) to evaluate the influence of line pollution on the determination of mass loss parameters. Let us note the general very good agreement between the positions and strengths of the Fe V lines and the absorption features polluting both the local stellar continuum (cf. the series of lines near λλ 1374, 1376, 1378, 1415 and 1420 Å) and the Si IV P Cygni profile (cf. the strong lines near λλ 1388, 1398, 1401, 1402, 1407 and 1409 Å).

2.2. C IV λλ *1548*, *1550 Å*

With the exception of five objects in the WNP atlas, all stars display in their spectra a P Cygni profile for the C IV resonance line transitions. Figure 1 illustrates the average C IV line profile as obtained for two independent sets of 50 spectra. We notice that unlike for Si IV, a main pollution caused by Fe IV lines occurs in this spectral range. The most noticeable feature is the strong depression of the star continuum on the red side of the C IV P Cygni profile due to the increasing density of Fe IV lines with wavelength. Also striking are the blends of Fe IV absorption lines near λλ 1527 and 1533 Å which affect a proper determination of the terminal velocity from the measurement of the blue edge of the C IV line profile (see also Figs. 3b–e in Blomme 1990). The narrow emission peak components which are often seen near the center of the C IV emission line profile (cf. Fig. 1 and Fig. 1 in Bernabeu et al. 1989) are also artefacts of the Fe IV line pollution.

2.3. He II λ *1640 Å*

Figure 3 represents a plot of the average spectral region near He II as obtained also from the spectra of all 98 stars. Let us notice that the presence of strong Fe IV lines near 1640 Å may affect the real strength of the He II λ 1640 line, specially if the latter one is weak.

© European Southern Observatory • Provided by the NASA Astrophysics Data System

1991A&A...247..469N

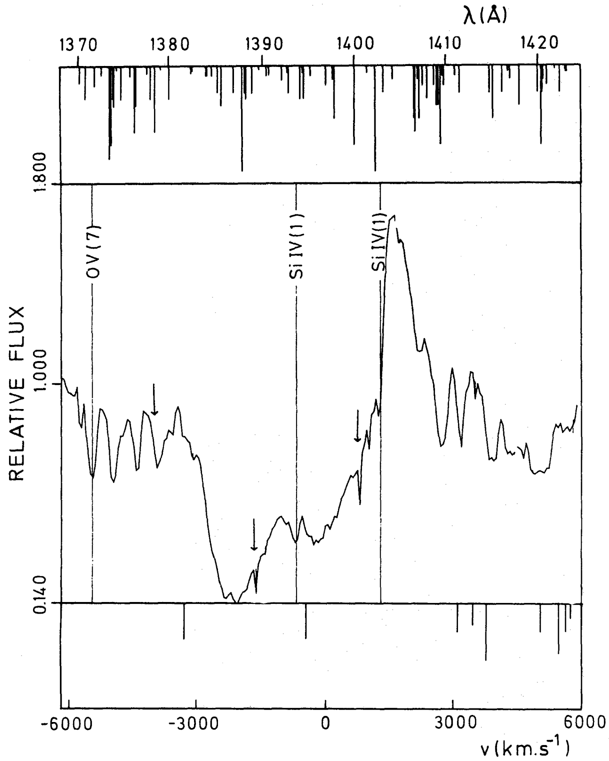

Fig. 2a. Representative Si IV P Cygni line profile for supergiant O-type stars as constructed from the average spectrum of 28 objects selected in the WNP atlas

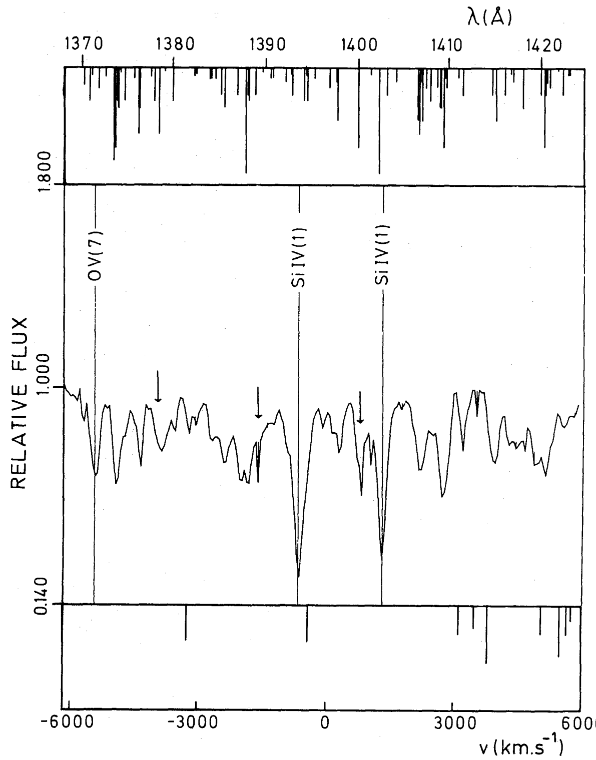

Fig. 2b. Same as Fig. 2a but for a sub-sample of 20 main-sequence and dwarf O-type stars

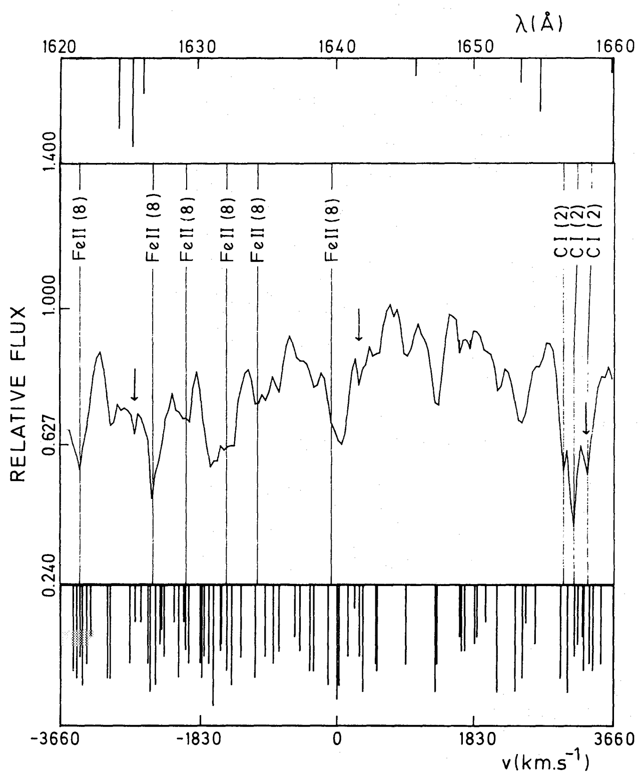

Fig. 3. Same as Fig. 1 (average of 100 spectra) but for the spectral region near the He II line transition

2.4. N IV λ 1718 Å

In the spectral region near N IV λ 1718 Å, as in the previous one, the density of Fe IV lines is quite high. In particular, there are blends of strong Fe IV lines near λλ 1718 and 1724 Å which perturb significantly the N IV absorption trough and the red wing of the emission component.

2.5. Conclusions

We have seen that in each of the Si IV, C IV, He II and N IV spectral regions, there is an essentially good correlation between the expected strengths of Fe IV and/or Fe V lines and the observed intensities of the polluting photospheric absorption lines. We may naturally wonder now: i) whether there is any influence of the stellar parameters on the intensities of these Fe IV and Fe V lines? and ii) what are the effects of the iron lines on the determination of the physical parameters characterizing the observed P Cygni profiles?

3. Influence of the stellar parameters on the observed intensities of the polluting iron lines

In order to test the possible effects of the effective temperature $T_{\rm eff}$ and of the stellar luminosity L_* on the observed intensities of Fe IV and Fe V lines in the spectra of the 98 stars compiled in WNP, we have constructed several (6) distinct groups of stars characterized by different average values of $T_{\rm eff}$ and L_*. The stellar parameters of these stars were taken from Howarth & Prinja (1989) and Groenewegen & Lamers (1989). We compared then the intensity of the Fe IV and Fe V lines in the average spectra of the six different

© European Southern Observatory • Provided by the NASA Astrophysics Data System

1991A&A...247..469N

groups of stars and report here the following points: i) the intensity of the Fe V lines increases with $\log(T_{\rm eff}) \in [4.46, 4.70]$ while the Fe IV lines present the opposite trend, ii) the strength of the Fe IV lines is quite insensitive to the stellar luminosity $\log(L_*) \in [4.50, 6.20]$, iii) while the same is true for the Fe V lines at temperatures in the range $\log(T_{\rm eff}) \geqslant 4.58$, the strength of the Fe V lines does also increase with $\log(L_*) \in [4.50, 6.20]$ for $\log(T_{\rm eff}) \leqslant 4.58$, and finally, iv) the absorption feature present at λ 1640 Å, and usually attributed to He II, shows the same behaviour with $T_{\rm eff}$ as the Fe IV lines. This supports again our previous claim that the strength of the He II λ 1640 line in the spectra of O-type stars may be possibly affected by the presence of Fe IV lines. We intend to investigate this point in a more quantitative way in the near future.

4. Influence of the Fe IV and Fe V lines on the determination of the physical parameters characterizing the observed P Cygni profiles

In this section, we shall first set up an approximate but very efficient numerical algorithm to correct observed P Cygni line profiles for the presence of underlying photospheric absorption lines.

4.1. A method for de-polluting P Cygni line profiles

In the framework of the Sobolev approximation used for the transfer of line radiation, we consider an expanding atmosphere around a central star of radius R_*, having a terminal velocity v_∞, in which two-level atoms scatter line radiation in a transition with rest frequency ν_{12}. In terms of the reduced velocity

$$X' = \frac{v(r)}{v_\infty},$$

$v(r)$ representing the radial velocity of the flow at a distance r from the center of the star, and considering the reduced frequency

$$X = \frac{\nu - \nu_{12}}{\nu_{12}} \frac{c}{v_\infty},$$

we know that only those atoms verifying the Doppler relation

$$X = -X'\mu$$

will interact with line radiation emitted from the stellar core at a frequency ν, along directions making an angle $\vartheta = \arccos(\mu)$ with respect to the radial direction. Defining the "photospheric absorption profile"

$$\Phi(X) = \frac{I_c(X)}{I_c},$$

where $I_c(X)$ and I_c represent respectively the intensities of the stellar continuum affected and (hypothetically) not affected by underlying photospheric absorption lines at a frequency X, it is straightforward to show that the expression of the source function S_{12}^{Φ} may be written as

$$S_{12}^{\Phi}(X') = \frac{\beta_{12}^{3,\Phi}(X')}{\beta_{12}^{1}(X')}$$

with

$$\beta_{12}^{3,\Phi} = \int_{4\pi W} \Phi(-X'\mu) \frac{(1-\mathrm{e}^{-\tau_{12}(X',\mu)})}{\tau_{12}(X',\mu)} \,\mathrm{d}\mu$$

and where $\beta_{12}^{1}(X')$ stands for the usual escape probability of a line photon in the expanding envelope (Surdej 1977). In the previous expression, τ_{12} represents the fictitious opacity of the atmosphere and $W(\simeq R_*^2/4r^2)$ the geometrical dilution factor. Since $W \ll 1$ in most parts of the atmosphere, the profile $\Phi(-X'\mu)$ can be conveniently approximated by $\Phi(-X')$ so that we may write

$$S_{12}^{\Phi}(X') \cong \Phi(-X')\, S_{12}(X'), \tag{1}$$

$S_{12}(X')$ being the source function that would have been calculated for the specific case of a flat stellar continuum (i.e. $I_c(X) \equiv I_c (=C^{\rm te})$).

Assuming that $\Phi(X) \neq 1$, let $E^{\Phi}(X)$ be the total amount of spectral energy, defined per frequency and solid angle units, radiated by the expanding atmosphere towards a fixed observer at a frequency $X \in [-1, +1]$. Following a similar procedure as in Surdej (1979), we easily find that

$$E^{\Phi}(X) = 2\pi \int_0^{r_{\max}} S_{12}^{\Phi}(X'(X,p))\,(1-\mathrm{e}^{-\tau_{12}(X',\mu)})\,p\,dp$$
$$+\begin{cases} 2\pi \int_0^{R_*} I_c(X)\,\mathrm{e}^{-\tau_{12}(X',\mu)}\,p\,dp, & \text{if } X<0 \\ E_c(X), & \text{if } X>0, \end{cases}$$

where $E_c(X)$ represents the unabsorbed flux emitted by the stellar core. In the above expression, the quantities S_{12}^{Φ} and τ_{12} are evaluated at the intersection of the surface of equal frequency X and the line of sight having an impact parameter p. With the help of relation (1) and taking into account the fact that the main contribution to the flux $E^{\Phi}(X)$ arises from regions located near the star, we can approximate the latter expression by

$$E^{\Phi}(X) = 2\pi\, \Phi(-X'(X,0)) \int_0^{R_{\max}} S_{12}(1-\mathrm{e}^{-\tau_{12}})\,p\,dp$$
$$+\begin{cases} 2\pi\,\Phi(X) I_c \int_0^{R_*} \mathrm{e}^{-\tau_{12}}\,p\,dp, & \text{if } X<0 \\ E_c(X), & \text{if } X>0. \end{cases} \tag{2}$$

At this stage, we shall consider the two following cases:

1) $X \leqslant 0$

For negative frequencies X, we have $X = -X'(X,0)$ and Eq. (2) simplifies to

$$E^{\Phi}(X) \cong \Phi(X)\, E(X), \tag{3}$$

$E(X)$ representing the flux that would be radiated if the stellar continuum was not affected by photospheric absorption lines.

2) $X \geqslant 0$

In this particular case, we have $X = X'(X,0)$ and Eq. (2) reduces to

$$E^{\Phi}(X) \simeq \Phi(-X)\,(E(X)-1) + E_c(X). \tag{4}$$

The presence of the term $\Phi(-X)$ in Eq. (4) accounts for an approximate treatment of the photospheric attenuation of the underlying stellar continuum as seen by the scattering atoms which do actually recede from the central star at velocities $X' \in [X, 1]$ and which contribute to the line flux $E^{\Phi}(X)$, at the observed frequency $X > 0$. A more sophisticated approach does indeed show that this term may be more adequately replaced in Eq. (4) by its average value $\langle \Phi(X) \rangle$ taken over the frequency range $X \in [-1, 0]$.

Finally, combining Eqs. (3) and (4), we find the form of the algorithm allowing one to correct an observed P Cygni profile for the presence of underlying photospheric absorption lines

© European Southern Observatory • Provided by the NASA Astrophysics Data System

1991A&A...247..469N

$$E(X) \cong E^{\Phi}(X)/\Phi(X), \qquad \text{if } X < 0,$$

and

$$E(X) \cong \frac{E^{\Phi}(X) - E_c(X)}{\langle \Phi(X<0) \rangle} + 1, \quad \text{if } X > 0. \tag{5}$$

4.2. Checks of the de-polluting numerical algorithm

We have tested extensively the numerical algorithm expressed in Eq. (5) as follows: we have first adopted the average spectrum of the five O-type stars showing no wind effects in the spectral region of C IV as the underlying stellar continuum $\Phi(X)$ (cf. the long dashed line spectrum in Fig. 4). By means of a numerical code of radiative transfer that will be described elsewhere (Nemry et al. 1991 b), we have then calculated for different velocity fields, opacity distributions, etc. the resulting polluted P Cygni line profiles (cf. the solid line spectrum in Fig. 4). The latter profiles have been then corrected for the presence of photospheric absorption lines by means of Eq. (5) (cf. the short dashed line profile in Fig. 4). Finally, we have also calculated the relevant P Cygni line profiles for the case $\Phi(X) = 1$ (cf. the crosses in Fig. 4). All our numerical results show that there is essentially a very good match between the corrected and the "un-polluted" line profiles. Since our numerical code used for the simulation of line profiles also gives the possibility to include turbulence effects in the expanding atmosphere as well as the finite structure of a resonance doublet (cf. the code described by Lamers et al. 1987), we have also applied our corrective method to such cases (cf. Figs. 5 and 6). It is interesting to note that Eq. (5) does also provide excellent results when turbulence effects and/or the finite structure of the resonance doublets are taken into account.

4.3. Numerical applications

In order to evaluate the effects of the polluting photospheric absorption lines on the estimate of mass loss rates, we have performed measurements of the first order moment W_1 for the Si IV and C IV profiles in different ways. For the Si IV line profiles, we made use of the average spectrum of the stars showing no wind effects (see Fig. 2b) to correct for the Fe V pollution in the average spectrum of the supergiant stars displaying well developed Si IV P Cygni profiles (see Fig. 2a). The result of applying our corrective method (cf. Eq. (5)) is illustrated in Fig. 7 where the solid line represents the original spectrum (cf. Fig. 2a) and where the dashed line corresponds to the corrected spectrum. This figure provides a good illustration of the Fe V lines blanketing effect. Three different

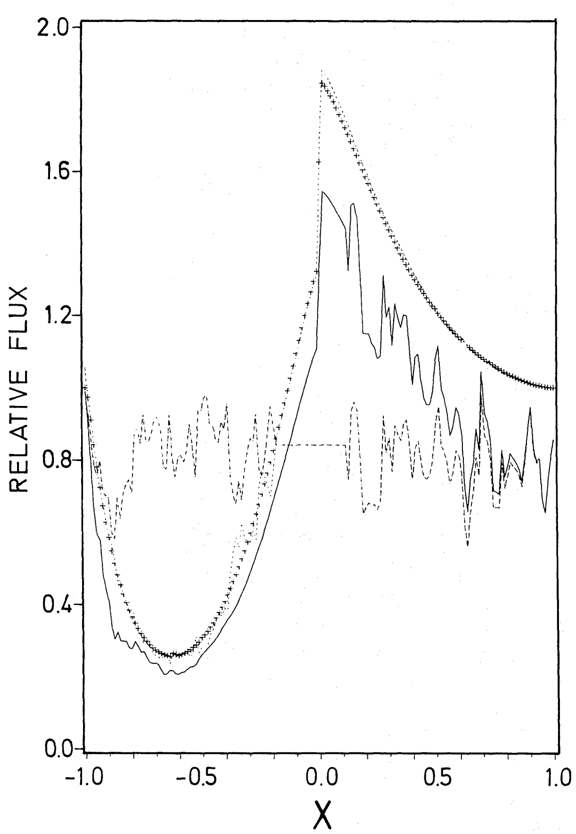

Fig. 4. The *long dashed line* curve illustrates an average underlying continuum $\Phi(X)$ constructed from the spectra of the five O-type stars showing no wind effects near the C IV line. The *solid line* represents the P Cygni line profile calculated with this underlying continuum $\Phi(X)$ under the Sobolev approximation for $v(r) \div (1 - R_*/r)$, $\tau^r_{12}(X) \div (1 - X)$ and $W_1^0 = 1$. The crosses represent the calculated P Cygni line profile for $\Phi(X) = 1$ and the *small dashed line* curve illustrates the result obtained after correction of the polluted line profile (*solid curve*) by means of Eq. (5)

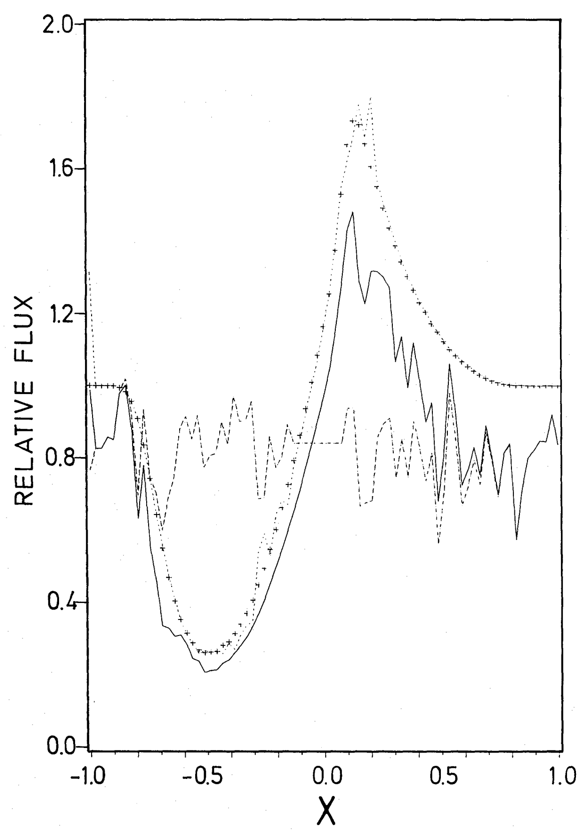

Fig. 5. Same as Fig. 4 but when turbulence effects ($\bar{u}/v_\infty = 0.1$) across the whole expanding atmosphere are taken into account

© European Southern Observatory • Provided by the NASA Astrophysics Data System

1991A&A...247..469N

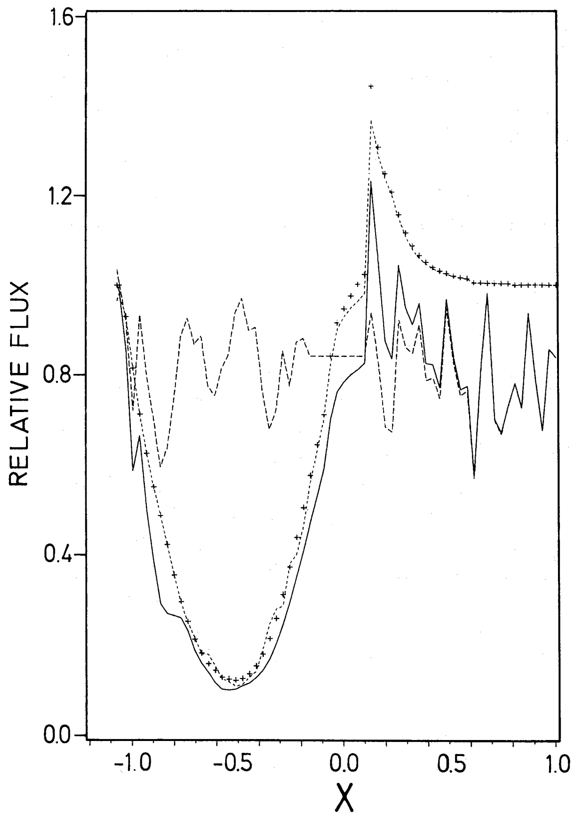

Fig. 6. Same as Fig. 4 but taking into account the structure of the resonance doublet. The Doppler velocity separation between the two line transitions was taken to be $\Delta v_{23} = 0.2\, v_\infty$ in the present case

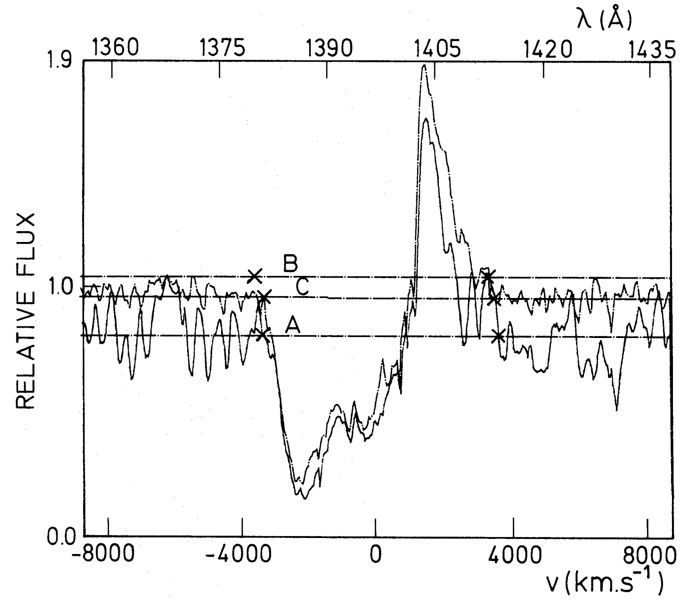

Fig. 7. The *solid line* in this figure represents the original Si IV P Cygni line profile of supergiant O-type stars as illustrated in Fig. 2a. The *dashed line* corresponds to the former line profile corrected for the pollution of photospheric absorption lines by means of the stellar spectrum in Fig. 2b, unaffected by stellar wind effects (see Text). The *horizontal lines* labelled *A*, *B*, and *C* represent different settings of the local stellar continuum used when measuring the first order moment W_1

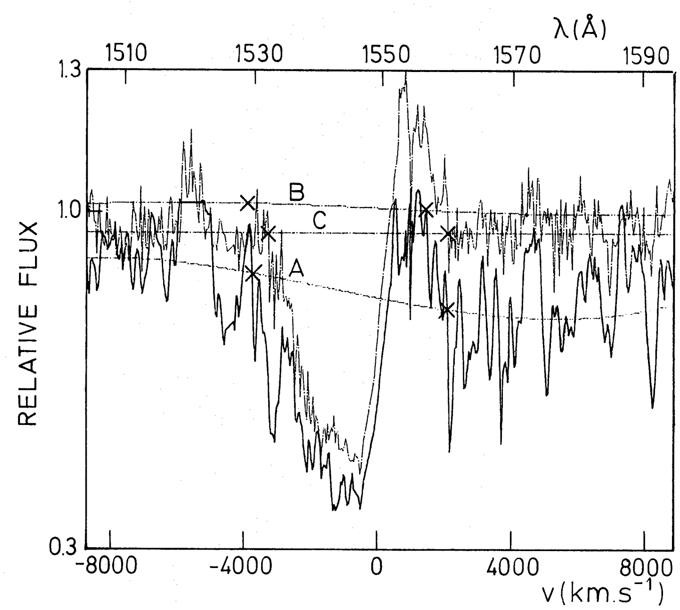

Fig. 8. As Fig. 7 but for the representative C IV P Cygni line profile of a sample of 20 main-sequence and dwarf O-type stars (see Text)

local continua, labelled A, B and C, have also been represented in this figure. The two first ones correspond to the uncorrected line profile. Continuum A was estimated assuming that one ignores totally the presence of the Fe V lines. Continuum B is represented by taking into account the presence of these lines. The latter was drawn just below the level of the highest points in the observed spectral continuum. Using these different continua, we assigned an edge velocity (cf. the positions of the crosses in Fig. 7). Then, we measured the first order moment W_1 (A & B) in both cases. Continuum C was drawn with respect to the corrected line profile and was used to measure the first order moment W_1 (C) considered as the most accurate one. It was easy in this way to determine the error affecting the mass loss rate estimates based upon the previous measurements. A similar treatment was applied to the average of the C IV line profiles illustrated in Fig. 1, using the average spectrum of the five stars showing no wind effect as the correcting spectrum. The results are shown in Fig. 8. Again, we can visualize the spectacular blanketing effect due to the Fe IV lines, increasing towards longer wavelengths. We then made use of the "$\log(W_1) - \log(W_1^0)$" diagrams calculated for resonance doublet P Cygni line profiles in the context of the Sobolev approximation (Surdej & Hutsemékers 1990). Recalling that the quantity W_1^0 is proportional to the product of the mass loss rate $\dot{M}$ and the average fractional abundance $\bar{n}$(level) of the ion under study, we have reported in Table 1 the relative uncertainties affecting the mass loss rate estimates for the Si IV, C IV line profiles illustrated in Figs. 7 and 8 as well as average values derived for a dozen of other representative cases in the WNP atlas. Since the relative uncertainties due to the Fe IV and Fe V line pollution in the mass loss rate estimates are typically of the order of 50%, but also possibly larger, it is imperative to take the polluted stellar continuum as a boundary condition when calculating theoretical P Cygni line profiles representative of O-type stars. Results summarized in Table 1 clearly show that it is not just sufficient to set a pseudo continuum below the level of the highest points in the observed spectral continuum to correct for the effects of underlying photospheric and interstellar absorption lines. Note that a first realistic approach to simulate P Cygni line profiles in the spectrum

© European Southern Observatory • Provided by the NASA Astrophysics Data System

1991A&A...247..469N

Table 1. Relative uncertainties affecting the estimate of mass loss rates $\dot{M}$ when no corrections for the pollution of Fe IV and Fe V lines are brought to the observed P Cygni profiles. The labels A, B and C refer to the different settings of the local stellar continuum (see text)

P Cygni line profile	$\left\lvert \frac{\dot{M}(A)-\dot{M}(C)}{\dot{M}(C)} \right\rvert$ (%)	$\left\lvert \frac{\dot{M}(B)-\dot{M}(C)}{\dot{M}(C)} \right\rvert$ (%)
Si IV as illustrated in Fig. 7	32	33
C IV as illustrated in Fig. 8	65	36
Other representative line profiles in the WNP atlas	54	45

of O-type stars using a photospheric input spectrum has been made by Gathier et al. (1981). A critical analysis of their method used for deriving empirical mass loss rates of O-type stars may be found in Surdej (1985).

5. Conclusions

In the present paper, we have studied and also abundantly illustrated the contamination effects of various P Cygni line profiles observed in the UV spectrum of O-type stars by photospheric absorption lines due to Fe^{3+} and Fe^{4+} ions. We find that ignoring these effects will generally result in appreciable and systematic errors (> 50%) of the mass loss rate estimates derived from the analysis of P Cygni line profiles such as C IV, Si IV, etc. We stress therefore the importance of "depolluting" all P Cygni line profiles observed in the ultraviolet spectral range before attempting any meaningful studies related to the determination of mass loss rates (and also possibly other physical parameters) of O-type stars.

Acknowledgements. It is a pleasure to thank the Astronomical Data Center at the NASA Goddard Space Flight Center for providing us a tape with the IUE O-type spectra from the atlas of Walborn, Nichols-Bohlin and Panek (1985). We are also very grateful to Dr. C. Leitherer for his interesting remarks and suggestions during the refereeing process of our paper.

References

Bernabeu G., Magazzù A., Stalio R., 1989, A&A 226, 215
Blades J.C., Wheatley J.M., Panagia N., Grewing M., Pettini M., Wamsteker W., 1988, ApJ 334, 308
Blomme R., 1990, A&A 229, 513
Bruhweiler F.C., Kondo Y., McCluskey G.E., 1981, ApJS 46, 255
Castor J.I., Lutz J.H., Seaton M.J., 1981, MNRAS 194, 547
Cerruti-Sola M., Perinotto M., 1985, ApJ 291, 237
Cerruti-Sola M., Perinotto M., 1989, ApJ 345, 339
Dean C.A., Bruhweiler F.C., 1985, ApJS 57, 133
Ekberg J.O., 1975, Phys. Scripta 12, 42
Ekberg J.O., Edlen B., 1978, Phys. Scripta 18, 107
Gathier R., Lamers H.J.G.L.M., Snow T.P., 1981, ApJ 247, 173
Groenewegen M.A.T., Lamers H.J.G.M.L., 1989, ApJS 79, 359
Groenewegen M.A.T., Lamers H.J.G.L.M., Pauldrach A.W.A., 1989, A&A 221, 78
Hamann W.-R., 1981, A&A 93, 353
Howarth I.D., Prinja R.K., 1989, ApJS 69, 527
Kelly R.L., Palumbo L.J., 1973, Atomic and ionic emission lines below 2000 angstroms, N&L Rept. No. 7599
Lamers H.J.G.L.M., Cerruti-Sola M., Perinotto M., 1987, ApJ 314, 726
Moore C.E., 1962, NBS Circ. 488, 4
Moore C.E., 1967, NSRDS-NBS3, 2
Moore C.E., 1970, NSRDS-NBS3, 3
Moore C.E., 1971, NSRDS-NBS3, 4
Moore C.E., 1975, NSRDS-NBS3, 5
Nemry F., Surdej J., Hernaiz A., 1991a (in preparation)
Nemry F., Hutsemékers D., Surdej J., 1991b (in preparation)
Striganov, Sventitskii, 1968, Tables of spectral lines of neutral and ionized atoms, Plenum, New York
Surdej J., 1977, A&A 60, 303
Surdej J., 1979, A&A 73, 1
Surdej J., 1982, Ap&SS 88, 31
Surdej J., 1983a, Ap&SS 90, 299
Surdej J., 1983b, A&A 127, 304
Surdej J., 1985, A&A 152, 361
Surdej J., Hutsemékers D., 1990, A&A 233, 141
Walborn N.R., Panek R.J., 1984, ApJ 280, L27
Walborn N.R., Nichols-Bohlin J., Panek R.J., 1985, International Ultraviolet Explorer Atlas of O-type Spectra from 1200 to 1900 Å, NASA RP-1155 (WNP)

© European Southern Observatory • Provided by the NASA Astrophysics Data System